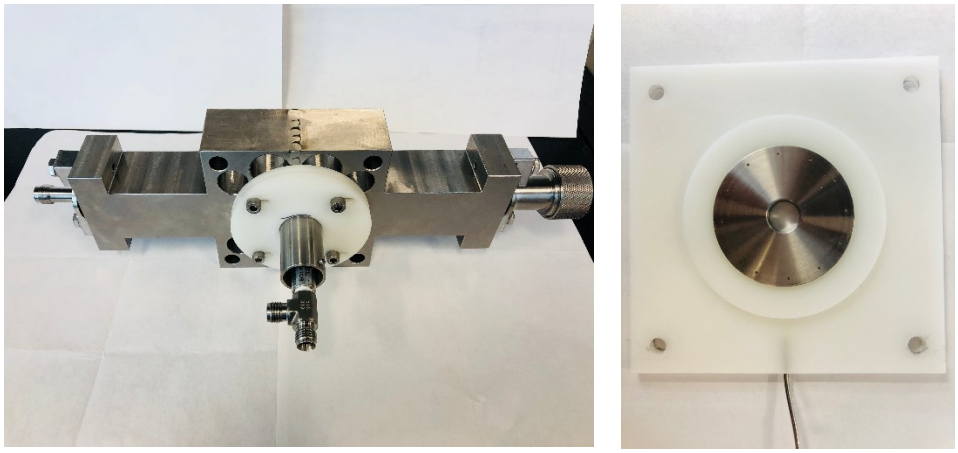

Figure S1. Photographs of the Transverse Ionization inlet (left) and the N_2 curtain gas plate (right).

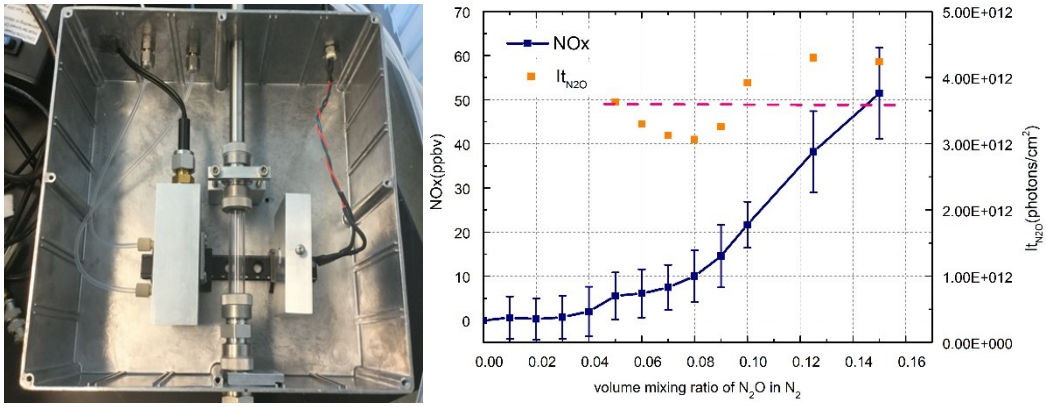

Figure S2. (Left) H_2SO_4 calibration system based on the design of Kurten et al. (Kurten et al., 2012). H_2SO_4 is generated by exposing known concentrations of gaseous SO_2, O_2, and H_2O to 185nm UV radiation produced by a mercury lamp (model 90-0012-01, Pen Ray) and a 185 nm bandpass filter (model XB32, 185BP20, Omega). Varying [H_2SO_4] was achieved under conditions of constant [SO_2] by varying [OH] in the system. OH is generated from the photolysis of water vapor. The water vapor concentration is calculated from the measured relative humidity (RH) and temperature. The [OH] in the system depends on both [H_2O] and the light strength, represented by *It* (amount of photons per cm^2), which is the product of the photon intensity *I* (amount of photons per second per cm^2) and the illumination time t_r (s).

(Right) Calibration of photodiode from the N_2O experiment. *It* was determined through chemical actinometry (N_2O to NOx conversion). The light strength was kept constant between photodiode calibration and H_2SO_4 calibration experiments, this was assured by measurements from a photodiode (model R5764, Hamamatsu) followed by an electrometer (model 485, Keithley). It_{N2O} was determined to be 3.85×10^{12} photons cm^{-2} when the photodiode current was 62nA. In the H_2SO_4 calibration experiment, all generated OH was transformed to H_2SO_4 within several milliseconds, 10% of [H_2SO_4] diffusion loss was applied to the 15 cm connection tube between the illumination area and the LTOF inlet. The generated [H_2SO_4] was constrained to above ~3×10^8 cm^{-3} because of the low detection limit of the RH sensor and the incomplete conversion of SO_3 to H_2SO_4 under low [OH]. (Kurten et al., 2012).

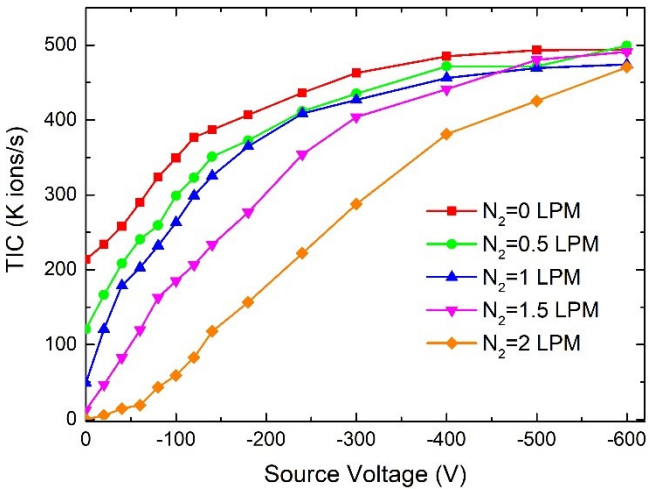

Figure S3. Total ion counts from the TI-CIMS as a function of ion source voltage at different curtain gas flow rates. As the ion source voltage increased, the voltage applied to the reaction chamber changed accordingly and always kept at half of the ion source voltage. A 1 LPM curtain gas flow rate and a -100V source voltage were used in our experiments.

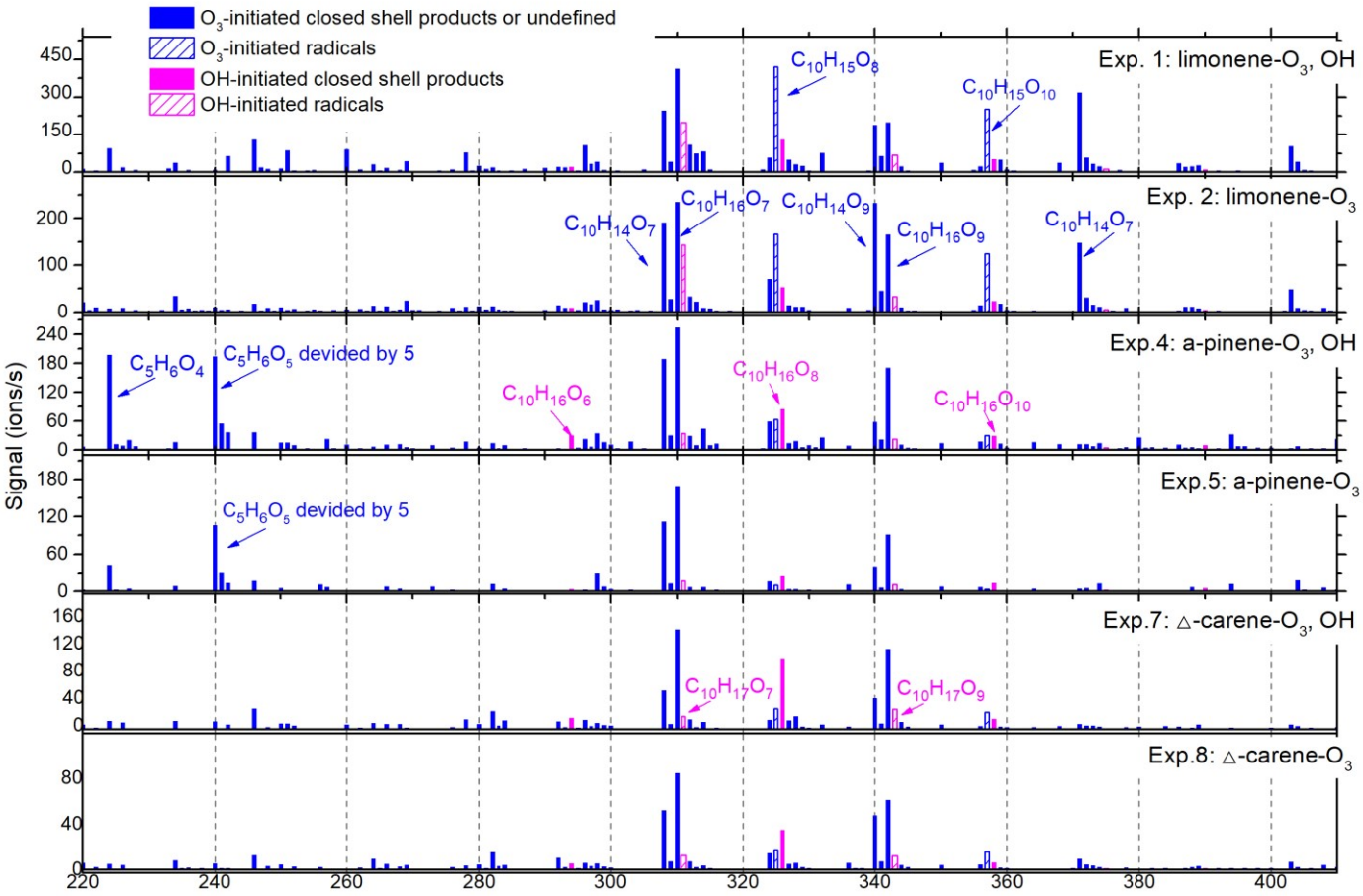

Figure S4. Averaged monomer and RO_2 radical mass spectra in six of the particle generation experiments. OH- and O_3-derived species were identified from previous studies (Jokinen et al., 2014). No significant differences were seen between experiments with and without OH scavengers. Peak labels are the identified neutral molecule, but the mass spectra show these compounds clustered with NO_3^- or $HNO_3NO_3^-$ reagent ions.

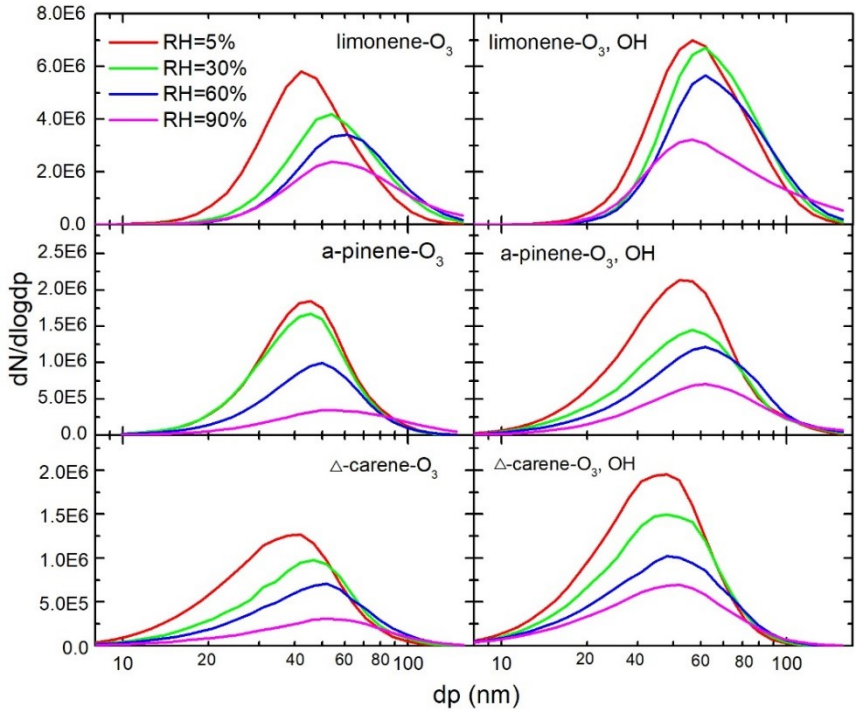

Figure S5. Averaged size distributions as a function of RH in each experiment.

Table S1. The Volatility of the major products were predicted with SIMPOL.1 (Pankow and Asher, 2008) and Molecular Corridor (298K) methods (Li et al., 2016).

	molecular	Osc	non-aromatic ring, b_4	C=C, b_5	-C=O-, b_9	-OH, b_7	-O-, b_{12}	-OOH, b_{27}	SIMPOL lgC*	M-corridor lgC*	Peak area
O_3-ROH	$C_{10}H_{16}O_7$	0.2	1	1	1	2	0	2	-3.46	0.5	412
	$C_{10}H_{16}O_9$	-0.2	1	1	1	2	0	3	-5.85	-1.85	199
O_3-ROOH	$C_{10}H_{16}O_6$	0.4	1	1	1	1	0	2	-1.31	1.58	22
	$C_{10}H_{16}O_8$	0	1	1	1	1	0	3	-3.69	-0.65	129
	$C_{10}H_{16}O_{10}$	-0.4	1	1	1	1	0	4	-6.08	-3.10	51
O_3-carbonyl	$C_{10}H_{14}O_7$	0	1	1	2	1	0	2	-2.22	0.50	245
	$C_{10}H_{14}O_9$	-0.4	1	1	2	1	0	3	-4.61	-1.85	187
O_3-dimer	$C_{20}H_{30}O_{10}$	0.5	2	2	2	2	1	2	-4.99	-4.98	65
	$C_{20}H_{30}O_{12}$	0.3	2	2	2	2	1	3	-7.40	-7.00	111
	$C_{20}H_{30}O_{14}$	0.1	2	2	2	2	1	4	-9.81	-9.16	64
OH-carbonyl	$C_{10}H_{16}O_6$	0.4	2	0	1	1	0	2	-1.11	1.58	22
	$C_{10}H_{16}O_8$	0	2	0	1	1	0	3	-3.60	-0.65	129
	$C_{10}H_{16}O_{10}$	-0.4	2	0	1	1	0	4	-5.99	-3.1	51
OH&O_3-dimer	$C_{20}H_{32}O_7$	0.9	3	1	1	2	1	1	-1.58	-2.32	18
	$C_{20}H_{32}O_9$	0.7	3	1	1	2	1	2	-3.98	-4.04	91
	$C_{20}H_{32}O_{11}$	0.5	3	1	1	2	1	3	-6.39	-5.97	84
	$C_{20}H_{32}O_{13}$	0.3	3	1	1	2	1	4	-8.80	-8.06	60
OH-dimer	$C_{20}H_{34}O_8$	0.9	4	0	0	2	1	2	-2.97	-3.15	--
	$C_{20}H_{34}O_{10}$	0.7	4	0	0	2	1	3	-5.38	-4.98	--
	$C_{20}H_{34}O_{12}$	0.5	4	0	0	2	1	4	-7.79	-7.00	--

[1]At T=298K, the parameters in SIMPOL.1 were b_0 = 1.842, b_4 = -0.021, b_5 = -0.108, b_7 = -2.183, b_9 = -0.937, b_{12} = -0.705, and b_{27} = -2.440 (Pankow and Asher, 2008).

[2]The functional groups used here were directly predicted from the proposed formation pathways in Figure 9 and did not include the intramolecular isomerization, like ring closure of unsaturated RO_2 (Berndt et al., 2016).

References cited

Berndt, T., Richters, S., Jokinen, T., Hyttinen, N., Kurtén, T., Otkjær, R. V., Kjaergaard, H. G., Stratmann, F., Herrmann, H., and Sipilä, M.: Hydroxyl radical-induced formation of highly oxidized organic compounds, Nature communications, 7, 13677, 2016.

Jokinen, T., Sipilä, M., Richters, S., Kerminen, V. M., Paasonen, P., Stratmann, F., Worsnop, D., Kulmala, M., Ehn, M., and Herrmann, H.: Rapid autoxidation forms highly oxidized RO2 radicals in the atmosphere, Angewandte Chemie International Edition, 53, 14596-14600, 2014.

Kurten, A., Rondo, L., Ehrhart, S., and Curtius, J.: Calibration of a Chemical Ionization Mass Spectrometer for the Measurement of Gaseous Sulfuric Acid, J Phys Chem A, 116, 6375-6386, 2012.

Li, Y., Pöschl, U., and Shiraiwa, M.: Molecular corridors and parameterizations of volatility in the chemical evolution of organic aerosols, Atmos Chem Phys, 16, 3327-3344, 2016.

Pankow, J. F., and Asher, W. E.: SIMPOL. 1: a simple group contribution method for predicting vapor pressures and enthalpies of vaporization of multifunctional organic compounds, Atmos Chem Phys, 8, 2773-2796, 2008.